

Supplemental material

Yeh et al., <https://doi.org/10.1085/jgp.201912360>

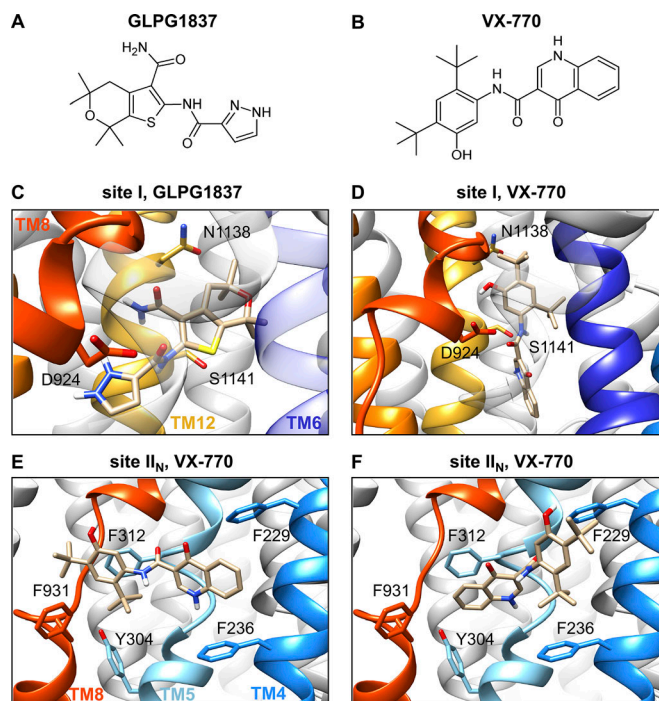


Figure S1. Chemical structures and docking modes of GLPG1837 and VX-770 in the cryo-EM structure of a phosphorylated, ATP-bound hCFTR. (A and B) Chemical structures of GLPG1837 (A) and VX-770 (B). (C and D) The docking mode of GLPG1837 (C) and VX-770 (D) at site I. The three residues subjected to functional studies (Figs. 2 and 3) are shown in the stick representation and colored by atom types (C, gold; N, blue; O, red; and S, yellow). (E and F) The two possible orientations of VX-770 at site II_N. This hydrophobic pocket composed of the five amino acid residues (labeled) within 5 Å of GLPG1837 (Fig. 5) can accommodate VX-770 in two different orientations of similar scores.

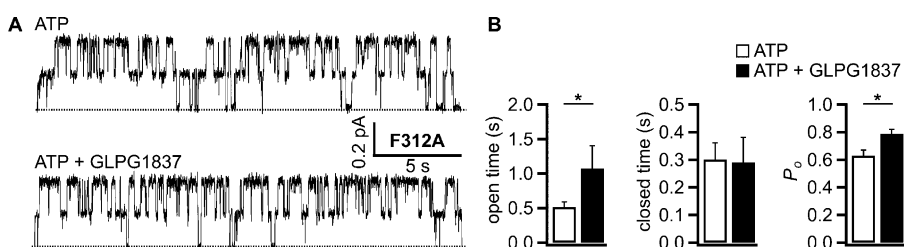


Figure S2. Effects of GLPG1837 on the microscopic channel activity of F312A-CFTR. (A) Representative recording from a patch containing two F312A-CFTR channels in the absence (top trace) or presence (bottom trace) of 20 μM GLPG1837. The dashed line marks the level when both channels are closed. (B) Comparison of kinetic parameters in the absence (blank bar) or presence (filled bar) of GLPG1837. Open time constant, closed time constant, and P_o : 514 ± 75 ms, 301 ± 61 ms, and 0.63 ± 0.04 without GLPG1837 ($n = 4$); 1,075 ± 327 ms, 293 ± 90 ms, and 0.79 ± 0.03 with GLPG1837. *, $P < 0.05$ (Student's *t* test). Error bars represent SEM.

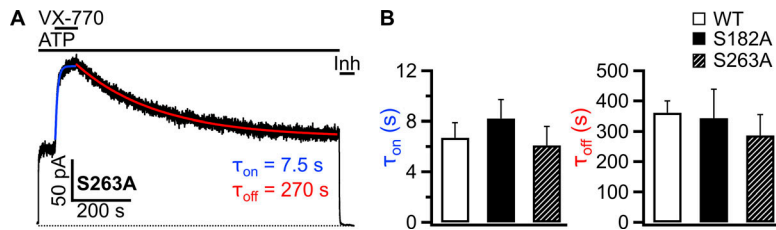


Figure S3. Responses of site IV mutants to application/washout of VX-770. **(A)** Representative macroscopic recording of S263A-CFTR in response to 200 nM VX-770. Single-exponential fitting was performed to yield the time constant of the rising phase (blue curve, τ_{on}) and the current decay (red curve, τ_{off}). **(B)** Summary of τ_{on} and τ_{off} of VX-770 for site IV mutants. As negative controls, the τ_{on} and τ_{off} for both S182A- and S263A-CFTR do not differ from that of WT-CFTR. τ_{on} : 6.7 ± 1.2 s (WT); 8.2 ± 1.5 s (S182A); 6.1 ± 1.5 s (S263A). τ_{off} : 361 ± 39 s (WT); 343 ± 96 s (S182A); 288 ± 68 s (S263A). ANOVA followed by Dunnett test was used to compare each mean against the mean of WT-CFTR. $n = 3$ for WT-CFTR. $n = 4$ for S182A- and S263A-CFTR. Error bars represent SEM.

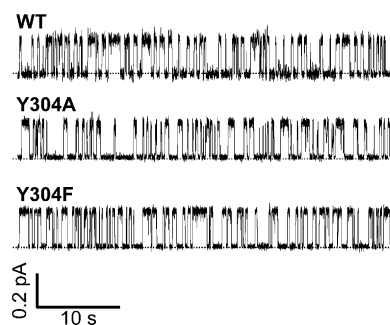


Figure S4. Single-channel activity of WT-, Y304A-, and Y304F-CFTR at 2 mM ATP. The bottom dashed line indicates closed state. Open time constant, closed time constant, and P_o : 397 ± 56 ms, 409 ± 35 ms, and 0.44 ± 0.02 for WT-CFTR ($n = 7$); 221 ± 20 ms, 467 ± 45 ms, and 0.31 ± 0.01 for Y304A-CFTR ($n = 5$); 412 ± 64 ms, 648 ± 108 ms, and 0.39 ± 0.03 for Y304F-CFTR ($n = 4$). Kinetic parameters for WT-CFTR are adopted from [Yeh et al., 2017](#).

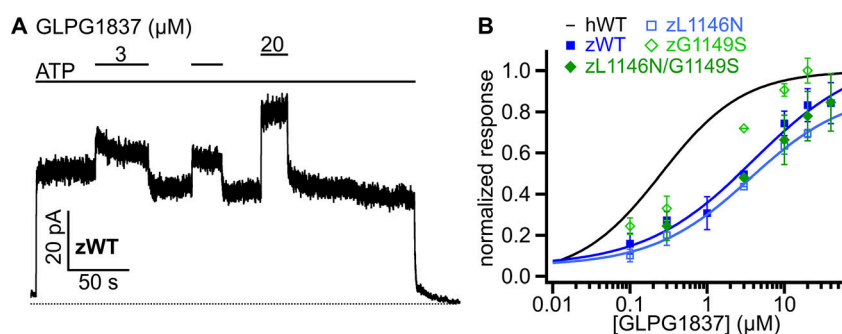


Figure S5. Dose-response relationships of GLPG1837 on zCFTR. **(A)** Effects of GLPG1837 on WT zCFTR (zWT). The percent increase of currents at 20 μ M GLPG1837 was twofold of that at 3 μ M GLPG1837, suggesting a decrease in the apparent affinity as compared with WT hCFTR (hWT), whose currents saturate at 3 μ M GLPG1837 ([Fig. 2 A](#)). **(B)** Rightward shift of the dose-response relationships of GLPG1837 on zCFTR. Hill equation fitting did not yield an accurate curve for the single mutant zG1149S and double mutant zL1146N/G1149S, as the currents have not reached saturation at the maximum concentrations we tested (see Materials and methods for details). EC₅₀ (μ M): 3.98 ± 1.74 (zWT) and 3.60 ± 1.92 (zL1146N). Error bars represent SEM.

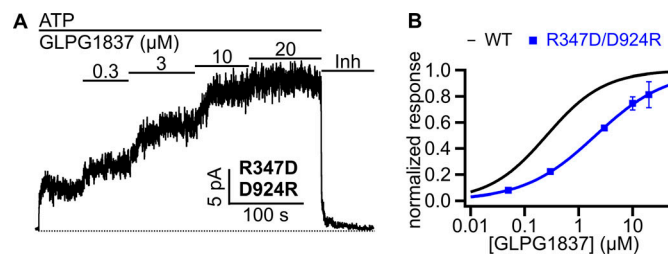


Figure S6. **Response of R347D/D924R-CFTR to GLPG1837.** **(A)** A representative recording showing the effect of GLPG1837 on R347D/D924R-CFTR, where the side chains of residues 347 and 924 are swapped. The maximum percent increase of current by GLPG1837 is $302 \pm 62\%$ (compare 115% for WT-CFTR; Table 1), a result indicating that the P_o of R347D/D924R-CFTR must be <0.25 ($1/4.02$). **(B)** Dose-response relationship of GLPG1837 for R347D/D924R-CFTR with an EC_{50} of $2.06 \pm 0.20 \mu\text{M}$. $n = 4$. Error bars represent SEM.

Reference

Yeh, H.I., Y. Sohma, K. Conrath, and T.C. Hwang. 2017. A common mechanism for CFTR potentiators. *J. Gen. Physiol.* 149:1105–1118. <https://doi.org/10.1085/jgp.201711886>